Simulation study of layer thickness and doping effects on PEA_2PbI_4-based perovskite solar cells

NIDHI SINGH[1], ANCHAL SRIVASTAVA[1], SUSHEEL KUMAR SINGH[2], K. C. DUBEY[3], SHOBHIT SHUKLA[4], R. K. SHUKLA[1,*]
[1]*Department of Physics, University of Lucknow, Lucknow-226007, India*
[2]*Department of Physics, Dr. S.M.N.R. University, Lucknow-226017, India*
[3]*Department of Physics, Shia P.G. College, Lucknow-226020, India*
[4]*Department of Information Technology, Dr. S.M.N.R. University, Lucknow-226017, India*

Perovskite materials are emerging as leading candidates for photovoltaic applications due to their remarkable optoelectronic properties and structural tunability. This study presents a numerical simulation of a 2D perovskite solar cell using PEA_2PbI_4 as the absorber, modeled with SCAPS-1D. The architecture FTO/ZnO:NR/PEA_2PbI_4/Spiro-OMeTAD/Au was optimized by adjusting absorber thickness (750 nm), ETL/HTL thicknesses (50 nm), doping levels, defect density (10^{15} cm^{-3}), and resistances. The optimized device achieved a peak PCE of 26.38% with excellent quantum efficiency and stability. These results highlight the importance of precise parameter tuning in enhancing 2D perovskite solar cell performance for scalable applications.

(Received May 22, 2025; accepted February 2, 2026)

Keywords: Perovskite, Solar Cell, PEA_2PbI_4, ZnO:NR, Spiro-OMeTAD, PCE

1. Introduction

In recent years, lead-based perovskite solar cells (PSCs) have emerged as highly promising candidates in the field of photovoltaics, primarily due to their remarkable power conversion efficiency (PCE). These materials have shown impressive performance enhancements, with reported efficiencies exceeding 25% [1–3], placing them among the leading technologies for next-generation solar energy systems. Among various lead-based options, two-dimensional (2D) perovskites have garnered significant attention owing to their excellent structural stability and tunable optoelectronic characteristics [4-5]. A particularly notable 2D perovskite is PEA_2PbI_4, which has proven to be a strong contender for the absorber layer in solar cell configurations [6]. PEA_2PbI_4 possesses a relatively narrow bandgap of around 1.7 eV, enabling it to harness a wider portion of the visible light spectrum compared to traditional materials like methylammonium lead iodide ($CH_3NH_3PbI_3$), which has a bandgap of 1.55 eV [7]. This broader absorption capability, coupled with efficient charge carrier generation, makes PEA_2PbI_4 a compelling material for developing sustainable and high-efficiency photovoltaic devices. However, despite its potential, in-depth investigations into the application of PEA_2PbI_4 as an absorber in solar cell architectures remain limited. Current literature lacks comprehensive evaluations of its performance metrics in device-level applications. In this context, theoretical simulations play a pivotal role by offering predictive insights and guiding the optimization of structural and material parameters [8]. This study aims to bridge that gap by theoretically analysing the performance of a solar cell structure incorporating PEA_2PbI_4 as the absorber. The chosen configuration, FTO/ZnO:NR/PEA_2PbI_4/Spiro-OMeTAD/Au, consists of fluorine-doped tin oxide (FTO) as the transparent conducting electrode, ZnO nanorods (ZnO:NR) as the electron transport layer (ETL), PEA_2PbI_4 as the absorber layer, Spiro-OMeTAD as the hole transport layer (HTL), and gold (Au) as the back contact [9]. By methodically varying critical parameters such as the thickness of each layer, doping concentrations, and defect densities, the study seeks to identify conditions that maximize device performance. Simulation results reveal that optimal efficiency is achieved when the ZnO:NR ETL and Spiro-OMeTAD HTL are each 50 nm thick, the PEA_2PbI_4 absorber layer is 750 nm thick, and the defect density within the absorber is 10^{15} cm^{-3}. Under these conditions, the solar cell exhibited a peak PCE of 26.38%. These results emphasize the potential of PEA_2PbI_4 - based solar cells to deliver high-efficiency outcomes while minimizing the environmental concerns typically associated with lead -containing materials. This work provides foundational knowledge that can aid researchers and industry professionals in developing more environmentally responsible and efficient solar technologies. By delivering a robust simulation-based performance assessment of PEA_2PbI_4 solar cells, this research lays the groundwork for experimental validation and further innovation. In summary, the continued advancement of 2D perovskite solar cells is vital for the transition to clean and sustainable energy systems. The combination of high PCE and a broader absorption spectrum positions PEA_2PbI_4 as a

leading alternative to conventional lead-based perovskites. Deepening our understanding of this material and refining its integration into photovoltaic architectures will be essential to achieving scalable, high-performance solar solutions. Future research should prioritize optimizing fabrication techniques and device structures while exploring the long-term stability and commercial scalability of PEA_2PbI_4 based devices.

2. Methodology

2.1. Research methodology

In this study, we employed the one-dimensional Solar Cell Capacitance Simulator (SCAPS), version 3.3.10, to analyse the performance of 2D perovskite solar cells. SCAPS is a widely used simulation tool in photovoltaic research, capable of modeling a variety of solar cell structures with high accuracy [10-13]. It solves key governing equations - namely the continuity equation, Poisson's equation, and semiconductor transport equations - which are essential for evaluating charge carrier dynamics, electric fields, and potential distributions within the device. These simulations help predict how structural and material parameters influence overall efficiency. SCAPS allows users to customize a broad range of input parameters, including bandgap energy, electron affinity, dielectric constant, layer thickness, doping concentrations, and defect densities. Additionally, it supports the simulation of devices under different operating conditions such as temperature and illumination intensity, making it a powerful tool for real-world performance assessments. In our work, SCAPS was used to perform a theoretical optimization of PEA_2PbI_4 - based solar cells by varying material and device parameters. This allowed us to identify performance-limiting factors and explore configurations that yield the highest power conversion efficiency. Overall, SCAPS served as an effective platform for simulating, analysing, and enhancing the photovoltaic behaviour of 2D perovskite devices.

2.2. Device structure and simulated parameters

To enhance efficiency, a five-layer perovskite solar cell (PSC) was designed using PEA_2PbI_4. The structure comprises FTO (transparent conductor), ZnO:NR (ETL), PEA_2PbI_4 (absorber), Spiro-OMeTAD (HTL), and gold (back contact). This architecture optimizes charge transport, reduces recombination, and improves light absorption. As shown in Fig. 1, it is tailored to boost performance by refining material properties and maximizing charge carrier collection.

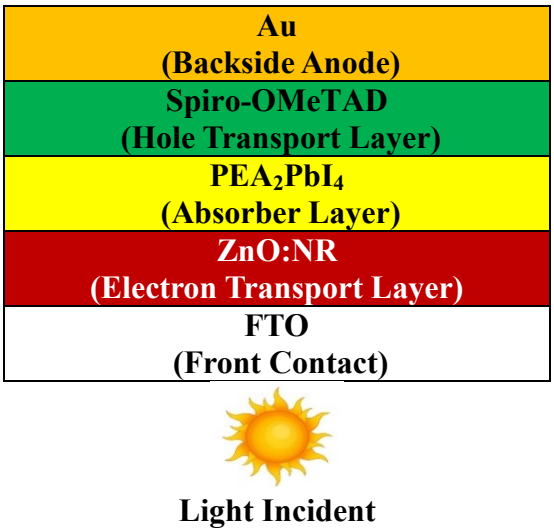

Fig. 1. Diagram of FTO/ZnO:NR/PEA_2PbI_4/Spiro-OMeTAD/Au based solar cell (colour online)

The initial physical parameters used for each layer of the proposed solar cell are listed in Table 1. These values, adopted from established studies [14-17], are essential for ensuring the simulation accurately mirrors real material characteristics and device behavior. Parameters such as thickness, band gap, electron affinity, doping concentration, and defect density directly affect charge generation, transport, and recombination, which in turn influence overall efficiency. Simulations were conducted at 300 K using the air mass 1.5 Global (AM1.5G) solar spectrum with an intensity of 1000 W/m² - conditions that closely approximate natural sunlight and standard testing environments. This setup enables meaningful comparison with experimental outcomes. Table 1 thus provides a robust foundation for evaluating and optimizing the performance of PEA_2PbI_4 - based perovskite solar cells under practical conditions.

Table 1. Initial material parameters for proposed solar cell used in SCAPS simulation

Physical Parameters	**Symbol**	**Unit**	FTO	Spiro-OMeTAD **(HTL)**	**PEA_2PbI_4**	**ZnO:NR (ETL)**
Thickness	**Th**	nm	400	100	400	100
Energy Band Gap	**E_g**	eV	3.5	3.0	1.7	3.47
Electron Affinity	**X**	eV	4.0	2.45	3.9	4.3
Dielectric Permittivity (Relative)	**ε_r**	-	9.0	3.0	25	9.0
Density of States at Valence Band	**N_V**	cm^{-3}	1×10^{18}	2.2×10^{18}	1×10^{18}	2×10^{18}
Density of States at Conduction Band	**N_C**	cm^{-3}	1.8×10^{19}	1.8×10^{19}	1×10^{18}	1.8×10^{20}
Thermal Velocity of Hole	**V_e**	cm/s	1×10^{7}	1×10^{7}	1×10^{7}	1×10^{7}
Thermal Velocity of electron	**V_h**	m/s	1×10^{7}	1×10^{7}	1×10^{7}	1×10^{7}
Electron Mobility	**μ_e**	$cm^2/V.s$	20	2×10^{-4}	25	100
Hole Mobility	**μ_h**	$cm^2/V.s$	10	2×10^{-4}	25	25
Uniform Shallow Donor Doping	**N_D**	cm^{-3}	2×10^{19}	0	1×10^{17}	1×10^{20}
Uniform Shallow Acceptor Doping	**N_A**	cm^{-3}	0	2×10^{18}	1×10^{15}	0
Defect Density	**N_t**	cm^{-3}	1×10^{15}	1×10^{15}	1×10^{15}	1×10^{15}
References			[14]	[15]	[16]	[17]

This study examines how key parameters influence the performance of the proposed PEA_2PbI_4 - based solar cell. Specifically, it evaluates the effects of layer thickness, donor (N_D) and acceptor (N_A) doping concentrations, and trap density (N_t) in each layer. Additionally, it investigates the impact of series resistance, shunt resistance, and temperature variations. The device performance is analyzed through current-voltage (I-V) characteristics, focusing on critical metrics such as short-circuit current density (J_{sc}), open-circuit voltage (V_{oc}), fill factor (FF), and power conversion efficiency (PCE). Using the initial material parameters listed in Table 1, the simulated results under standard conditions - 300 K and AM1.5G illumination - yield V_{oc} = 0.91 V, J_{sc} = 31.05 mA/cm², FF = 63.93%, and an overall PCE of 18.00%, reflecting a solid baseline for further optimization.

3. Results

3.1. Optimization of thickness of Absorber layer, PEA_2PbI_4

The absorber layer plays a crucial role in solar cell efficiency by capturing sunlight and generating electron-hole pairs for energy conversion. Optimizing its thickness is essential for maximizing performance. As shown in Fig. 2, photovoltaic parameters such as V_{oc}, J_{sc}, FF, and PCE were analyzed for PEA_2PbI_4 thicknesses ranging from 200 to 900 nm. The PCE reached a maximum of 21.65% at 750 nm, attributed to enhanced light absorption and carrier generation. Beyond this thickness, increased recombination reduces efficiency [18-21]. J_{sc} slightly declined from 18.93 to 18.89 mA/cm², and V_{oc} from 1.41 to 1.40 V, while FF rises from 79.65 to 81.47% [22].

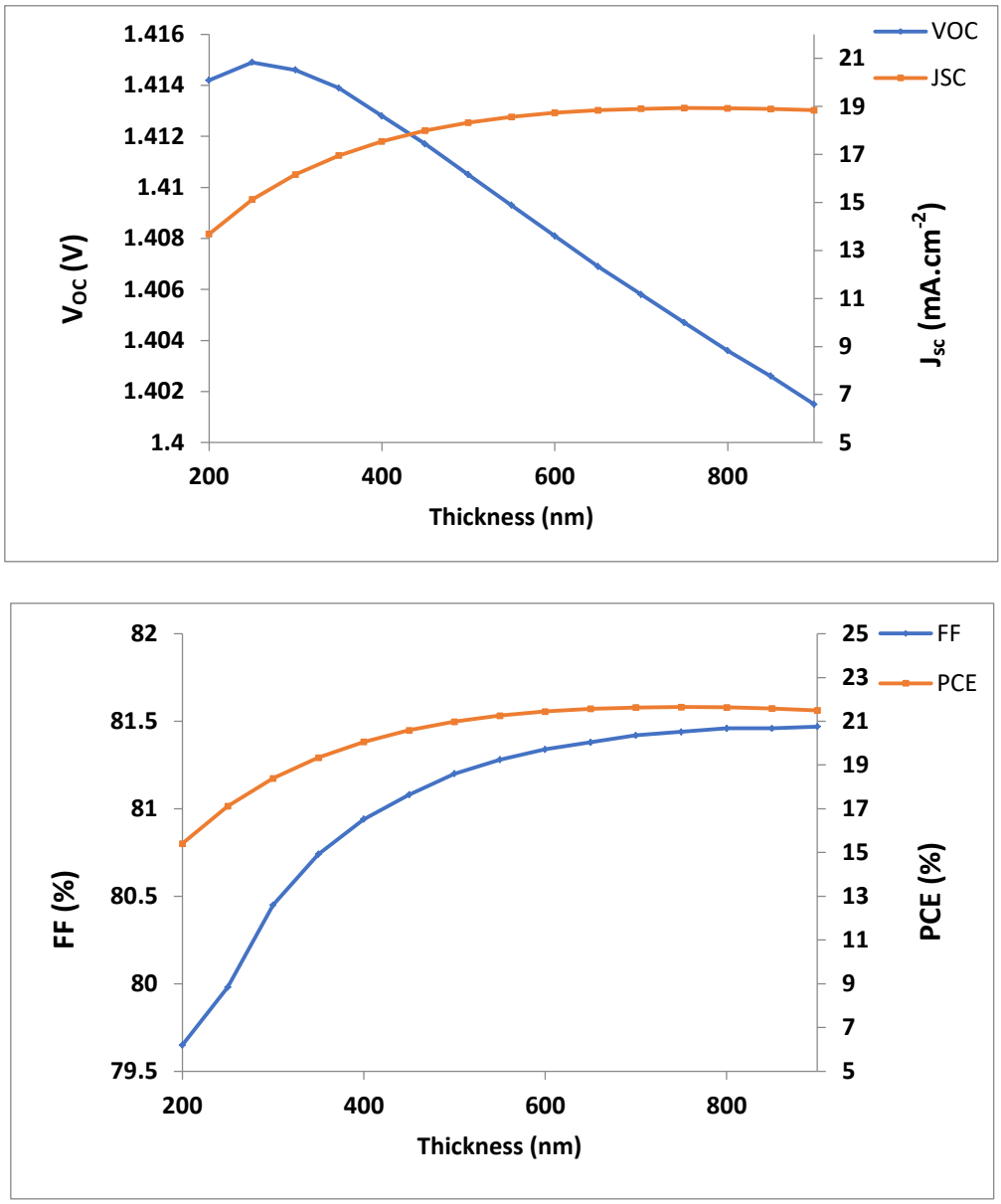

Fig. 2. Variation of the thickness PEA_2PbI_4 layer on simulated parameters of solar cell (colour online)

3.2. Optimization of donor density (N_D) of PEA_2PbI_4 layer

The effect of uniform shallow donor density in the PEA_2PbI_4 absorber layer was analyzed to assess its influence on solar cell performance. Photovoltaic parameters including V_{oc}, J_{sc}, FF, and PCE were examined across a donor concentration range of 10^{16} to 10^{20} cm^{-3}. As shown in Fig. 3, changes in donor concentration notably impact these parameters. The power conversion efficiency (PCE) reaches its maximum of approximately 25.33% at a donor density of 1×10^{20} cm^{-3}. With increasing donor concentration, V_{oc} rises from 1.34 to 1.58 V, J_{sc} slightly decreases from 20.66 to 18.75 mA/cm², and FF improves from 74.17% to 85.21%.

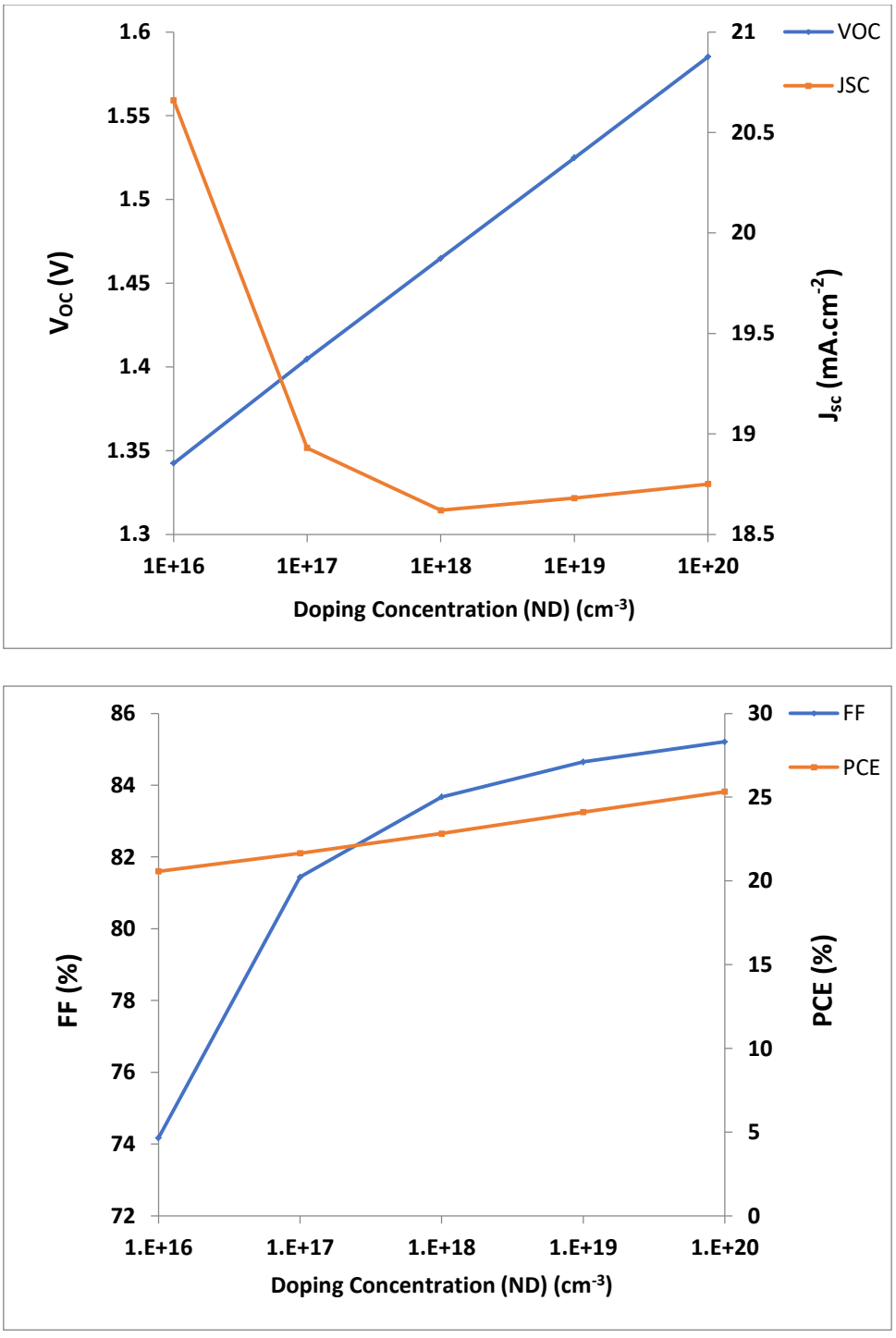

Fig. 3. Effect of the donor density (N_D) of PEA_2PbI_4 layer on simulated parameters of solar cell (colour online)

3.3. Optimization of acceptor density (N_A) of PEA_2PbI_4 layer

This section analyses the effect of varying uniform shallow acceptor density in the PEA_2PbI_4 absorber layer on solar cell performance. Key photovoltaic parameters - V_{oc}, J_{sc}, FF, and PCE - were studied across an acceptor concentration range from 10^{11} to 10^{19} cm^{-3}. As illustrated in Fig. 4, the highest PCE of approximately 25.33% is achieved at 10^{20} cm^{-3}. Notably, J_{sc} remains unaffected by changes in acceptor concentration, while other parameters show significant variation, enhancing overall efficiency.

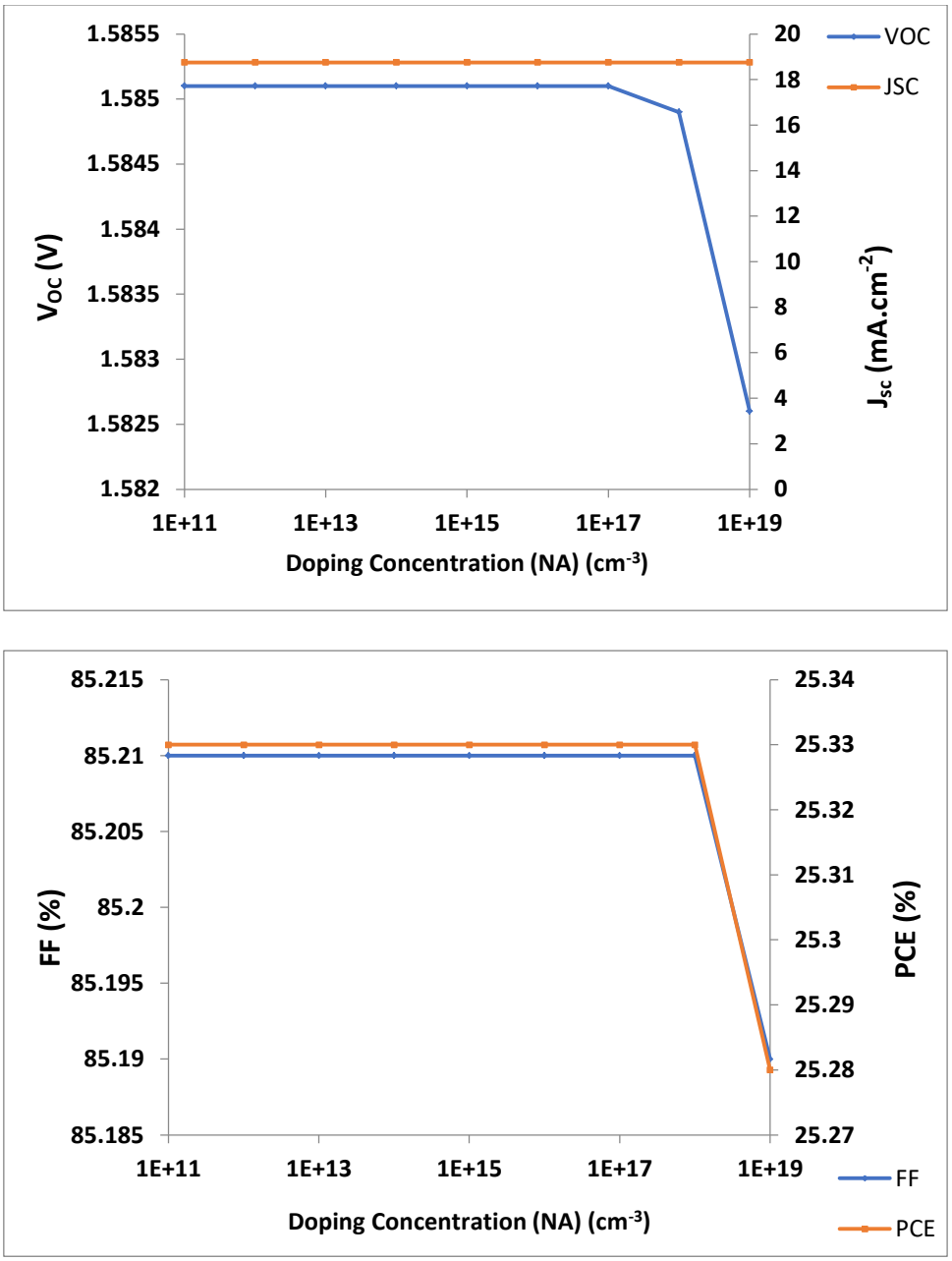

Fig. 4. Effect of the acceptor density (N_A) of PEA_2PbI_4 layer on simulated parameters of solar cell (colour online)

3.4. Optimization of thickness of ZnO:NR (ETL)

The ZnO:NR layer plays a vital role in facilitating charge transport and light transmission within the solar cell. Fig. 5 illustrates the effect of varying its thickness between 25 and 400 nm. As thickness increases, performance declines due to hindered charge transport. Optimal efficiency is achieved at a 50 nm thickness, yielding V_{oc} = 1.58 V, J_{sc} = 18.21 mA/cm², FF = 85.21%, and PCE = 25.34%. A thinner ETL enhances charge extraction and overall device efficiency.

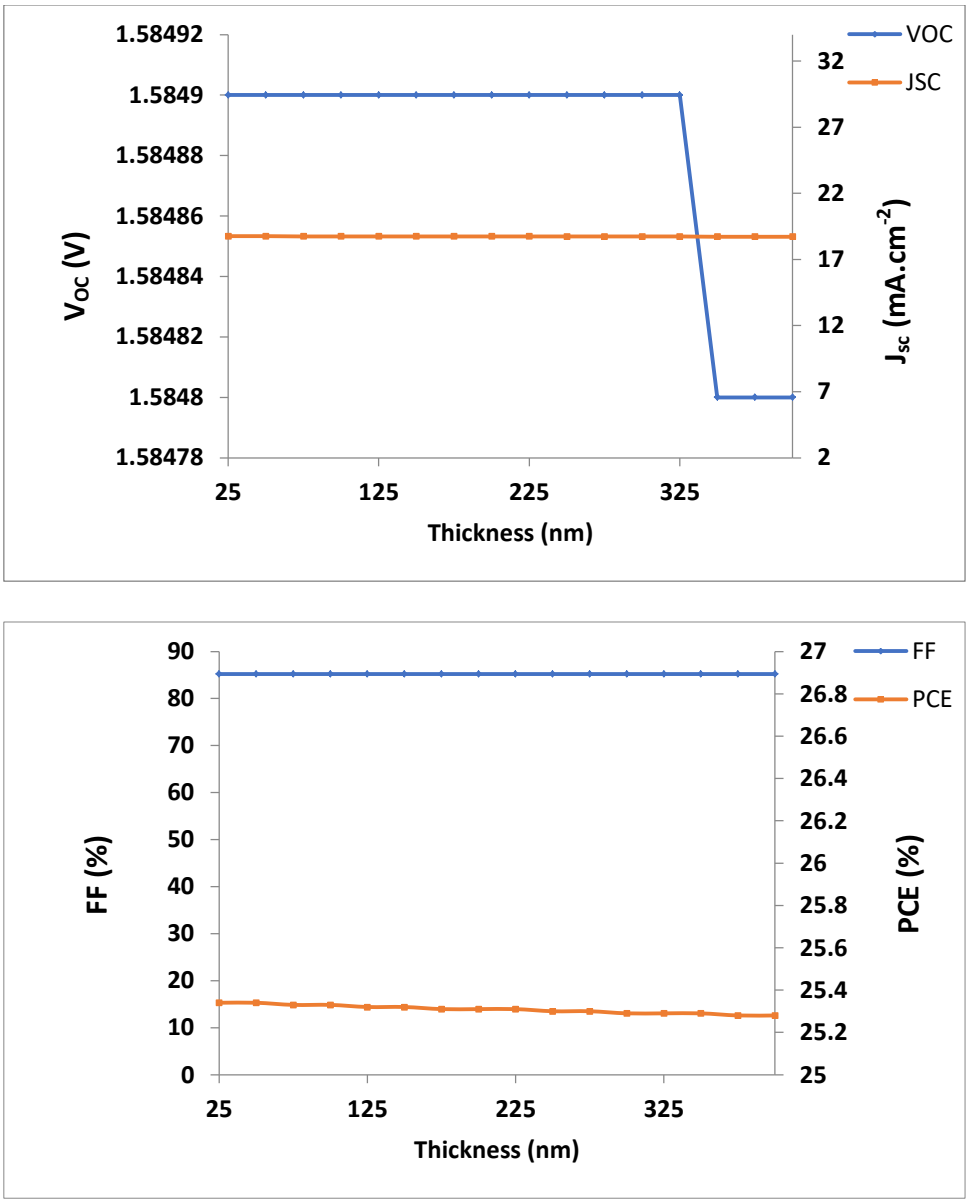

Fig. 5. Effect of the thickness of ETL (ZnO:NR) on simulated parameters of solar cell (colour online)

3.5. Optimization of donor doping concentration (N_D) of ETL (ZnO:NR)

To assess the impact of doping concentration on perovskite solar cell (PSC) performance, donor impurity concentration (N_D) was varied from 10^{11} to 10^{20} cm^{-3}. Fig. 6 demonstrates a slight increase in power conversion efficiency (PCE) from 25.24 to 25.34% as N_D rises. This improvement results from reduced series resistance and enhanced optical conductivity in the electron transport material (ETM). The optimal doping level of 10^{20} cm^{-3} yields PCE = 25.34%, J_{sc} = 18.76 mA/cm^2, V_{oc} = 1.58 V, and FF = 85.21%. Lower Auger recombination and quenching losses below this concentration highlight the importance of doping optimization for improved charge transport and efficiency.

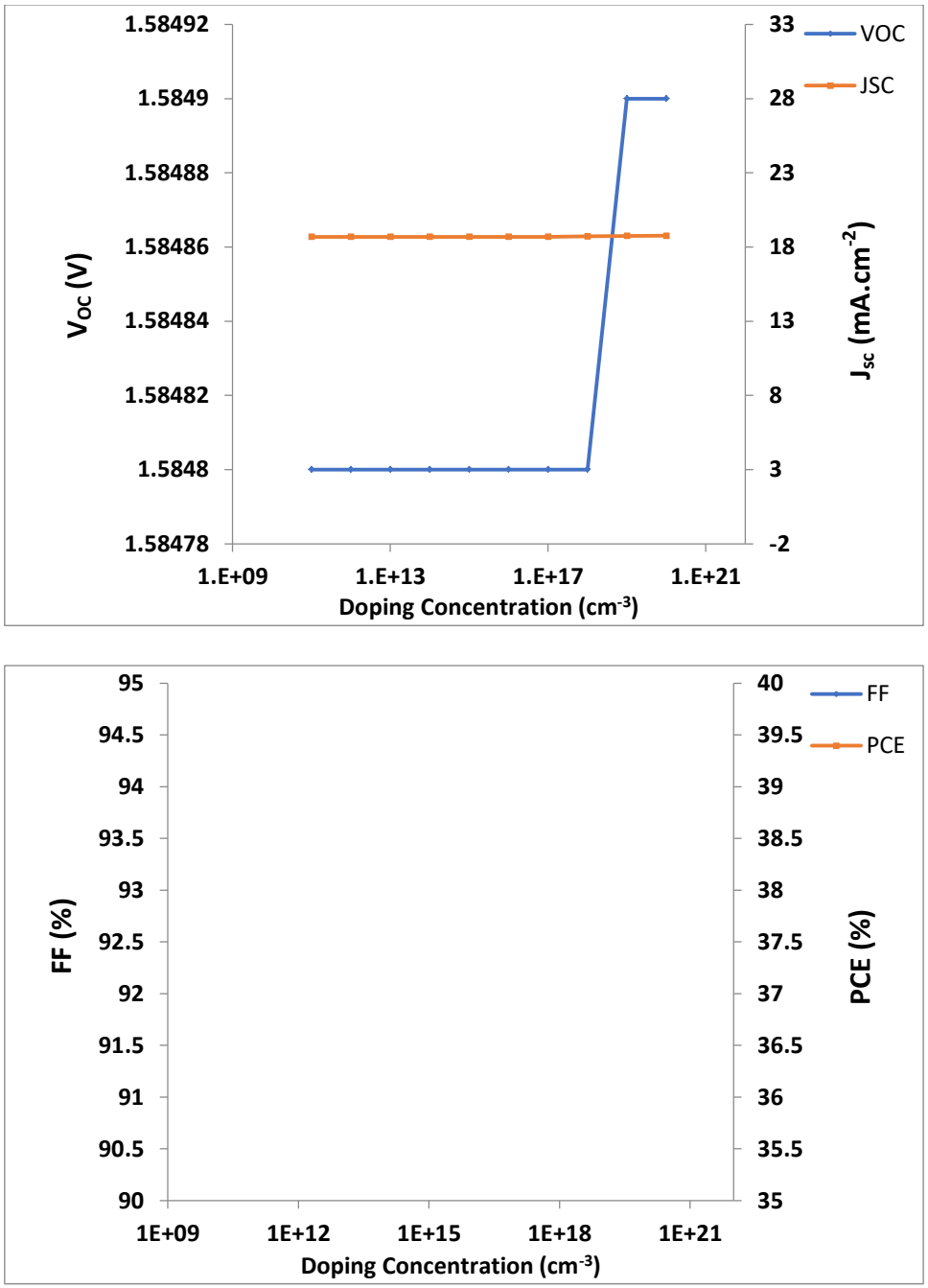

Fig. 6. Variation of doping concentration of ETL (ZnO:NR) on the simulated parameters of solar cell (colour online)

3.6. Optimization of defect density (N_t) of ETL, ZnO:NR

Defect density (N_t) in the ZnO:NR electron transport layer (ETL) significantly influences perovskite solar cell performance. Higher N_t causes increased electron and hole trapping, leading to greater recombination losses and reduced optoelectronic quality. As N_t increases from 10^{11} to 10^{20} cm^{-3}, power conversion efficiency (PCE) decreases from 25.34 to 25.24% (Fig. 7). This reduction underscores the critical need to minimize defects in the ETL to enhance charge transport, efficiency, and device stability.

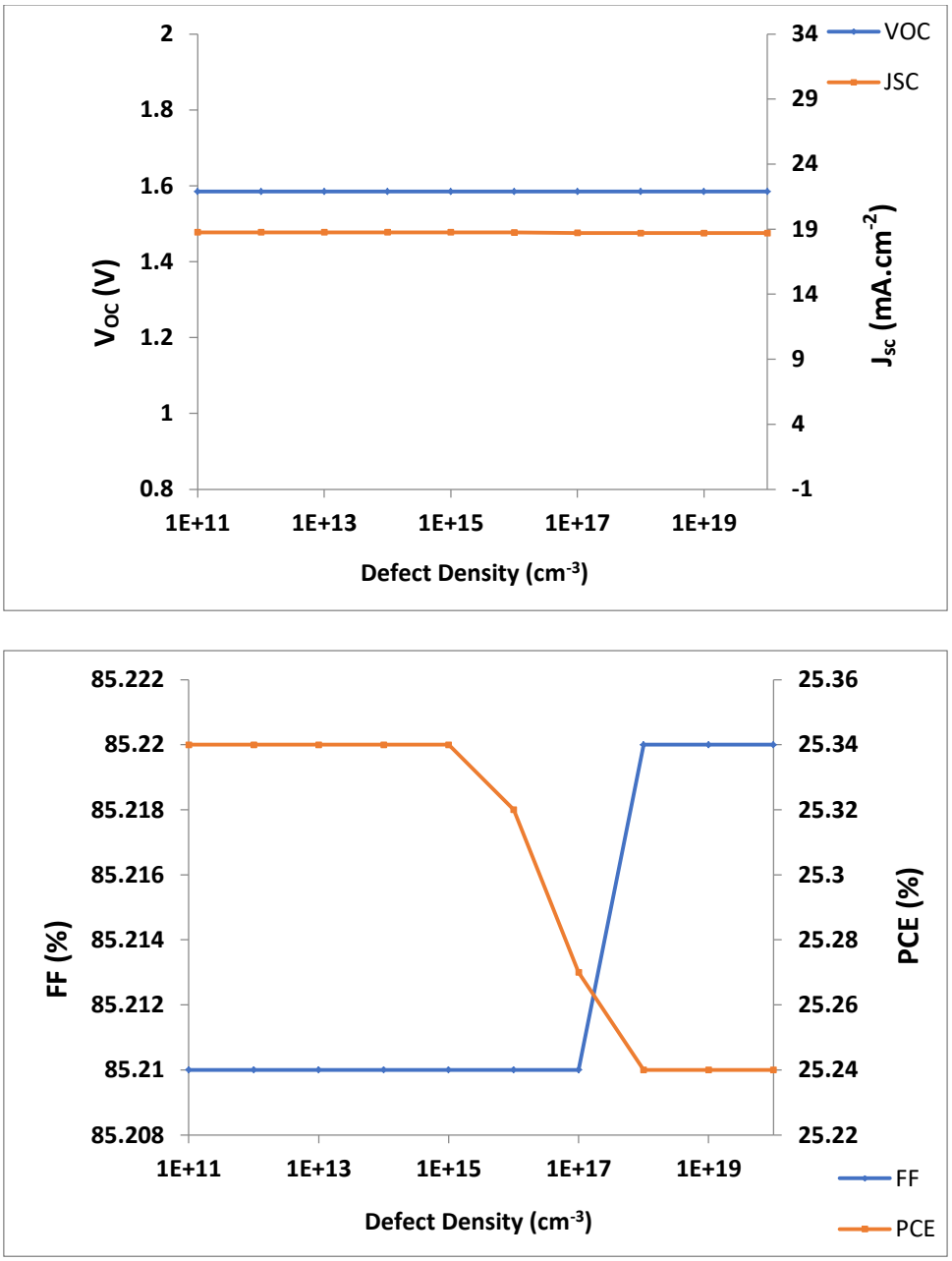

Fig. 7. Variation of the defect density of ETL (ZnO:NR) on simulated parameters of solar cell (colour online)

3.7. Optimization of thickness of HTL (Spiro-OMeTAD)

The efficiency of perovskite solar cells (PSCs) heavily relies on the electron and hole transport layers (ETL and HTL), where their thickness plays a crucial role in charge transport and overall device performance. Fig. 8 illustrates how varying the thickness of Spiro-OMeTAD (HTL) affects key parameters such as V_{oc}, J_{sc}, FF, and PCE. Thin HTLs may develop micro-pinholes, leading to direct absorber-electrode contact, while excessively thick HTLs increase series resistance (R_s), reducing efficiency. The study identifies 50 nm as the optimal HTL thickness, where PCE peaks. Beyond 50 nm, PCE declines to 25.17%, with V_{oc} and J_{sc} remaining stable and FF slightly dropping from 85.33 to 84.63%.

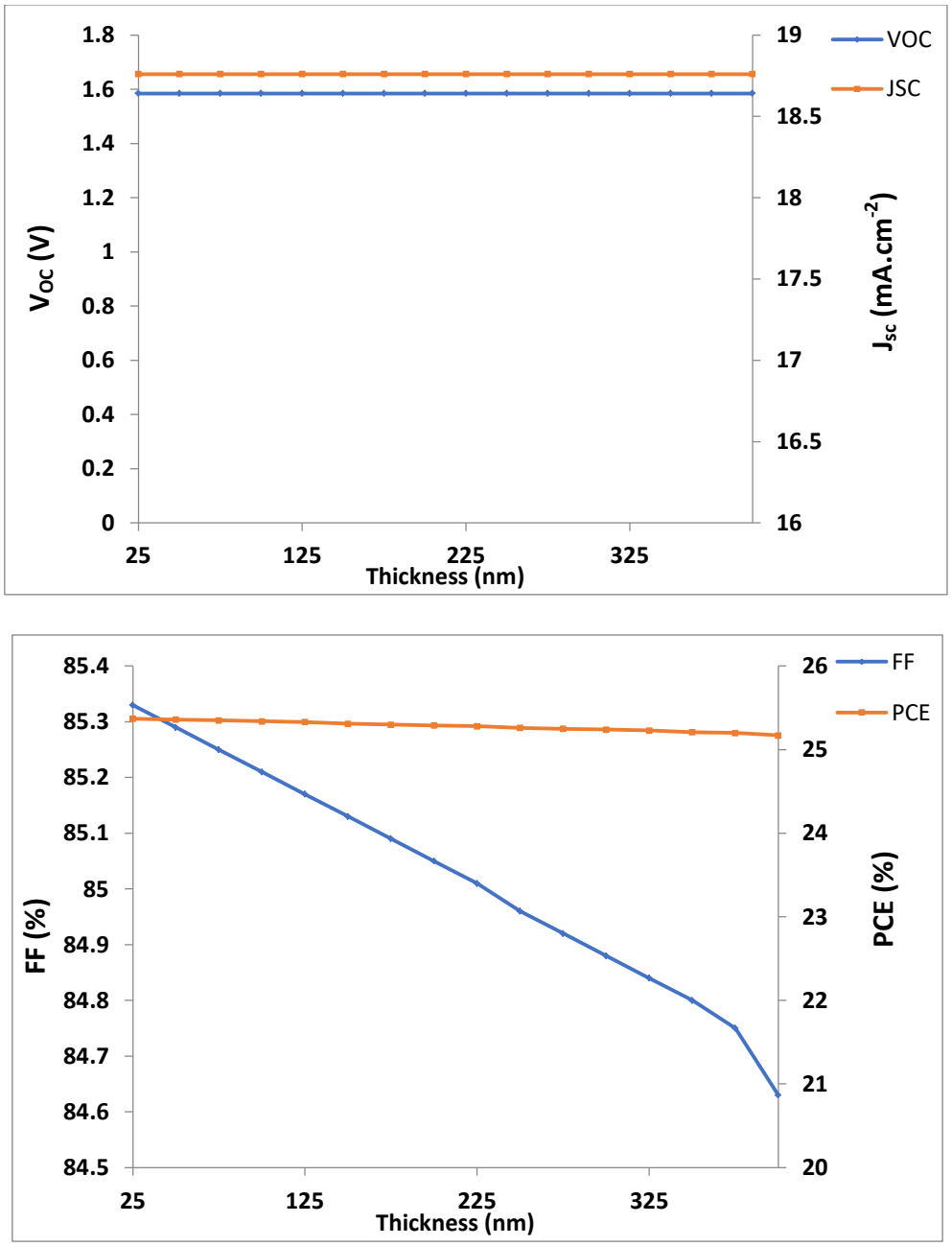

Fig. 8. Variation of the simulated parameters with the thickness of HTL (Spiro-OMeTAD) (colour online)

3.8. Optimization of doping concentration (N_A) of HTL (Spiro-OMeTAD)

The impact of acceptor impurity concentration (N_A) on perovskite solar cell (PSC) performance was analyzed from 10^{11} to 10^{20} cm^{-3}. Fig. 9 indicates minimal effect on overall efficiency. The optimized values are PCE = 26.38%, J_{sc} = 18.77 mA/cm^2, V_{oc} = 1.58 V, and FF = 88.78%. An N_A of 10^{20} cm^{-3} was chosen for further studies, providing stable and optimal performance.

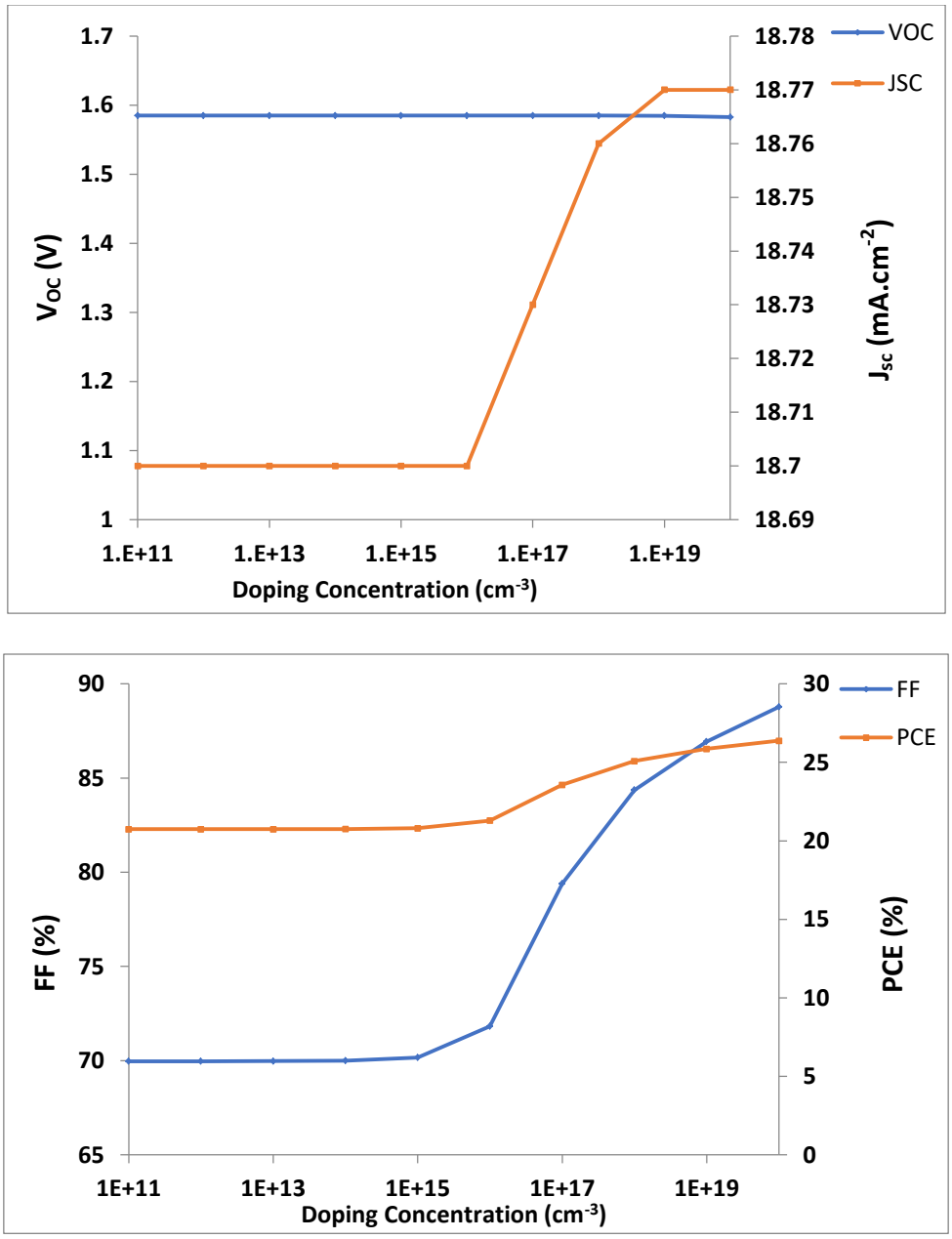

Fig. 9. Variation of the simulated parameters with the doping concentration of HTL (Spiro-OMeTAD) (colour online)

3.9. Effect of temperature

Understanding the effect of temperature on solar cell performance is essential for evaluating device stability and efficiency. We investigated temperatures ranging from 300 to 600 K and observed a significant decrease in power conversion efficiency (PCE), dropping from 26.38 % at 300 K to 23.20 % at 600 K, as shown in Fig. 10. This reduction is attributed to shorter charge carrier diffusion lengths, thermal stress-induced defects, and increased recombination rates, all contributing to diminish efficiency. Additionally, the open-circuit voltage (V_{oc}) declines from 1.58 to 1.36 V, while the short-circuit current density (J_{sc}) slightly increases from 18.77 to 20.32 mA/cm². Meanwhile, the fill factor (FF) decreases from 88.78 to 84.15% as temperature rises, highlighting the challenges of high-temperature operation.

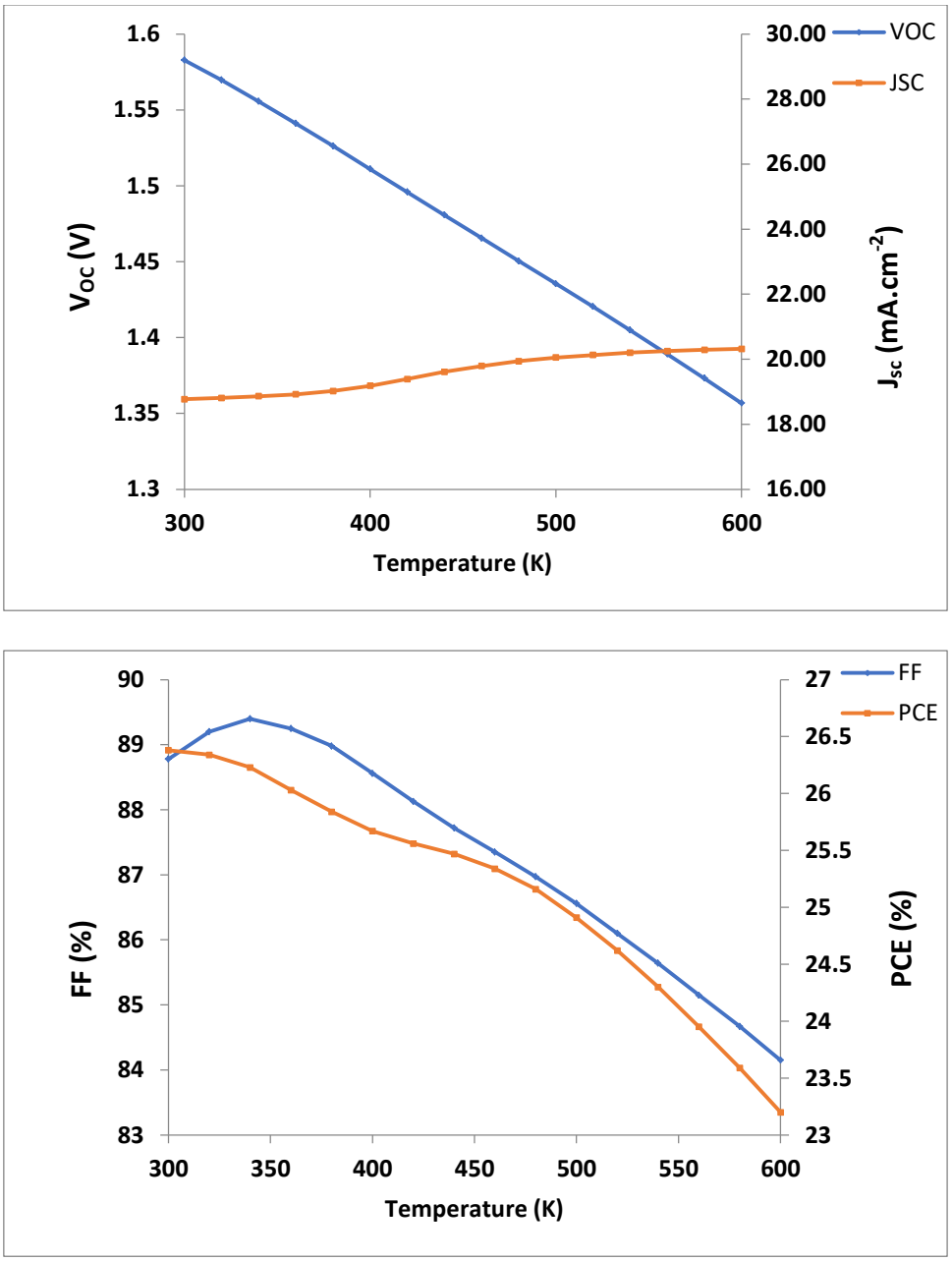

Fig. 10. Variation of the simulated parameters with the temperature (colour online)

3.10. Effect of series resistance

In perovskite solar cells (PSCs), series resistance (R_s) arises from material layers, interface barriers, charge-collecting interlayers, and metal contacts, while shunt resistance is caused by leakage paths such as recombination losses and pinholes in the active layer. As R_s increases, short-circuit current density (J_{sc}) and open-circuit voltage (V_{oc}) remain constant due to restricted current flow, but power conversion efficiency (PCE) decreases. To study R_s's effect, it was varied from 0 to 10 Ω·cm². Fig. 11 shows PCE drops from 26.39 to 23.00% as R_s rises, accompanied by a reduction in fill factor (FF). Optimal performance was achieved at R_s = 0 Ω·cm², emphasizing the need to minimize series resistance for maximum PSC efficiency.

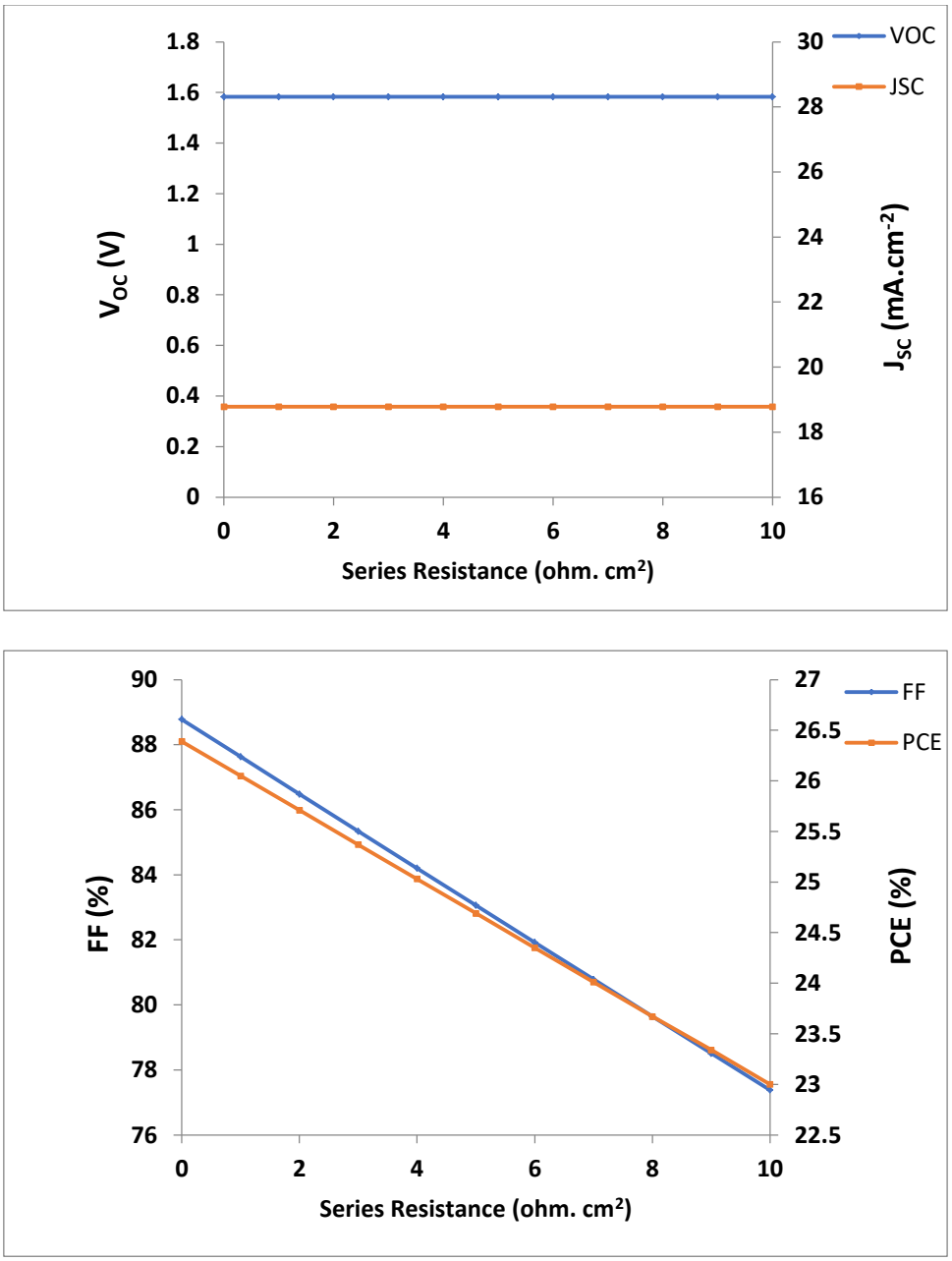

Fig. 11. Effect of the simulated parameters with the series resistance (colour online)

3.11. Effect of shunt resistance

Fig. 12 illustrates the impact of varying shunt resistance (R_{sh}) from 10^1 to 10^{10} Ω·cm² on solar cell performance. Open-circuit voltage (V_{oc}), power conversion efficiency (PCE), and fill factor (FF) increase sharply between 10^2 and 10^6 Ω·cm², then level off, while short-circuit current density (J_{sc}) remains unchanged. The efficiency improvement primarily results from the rise in FF. The optimal shunt resistance for maximum performance is 10^6 Ω·cm², ensuring peak efficiency in the proposed perovskite solar cells.

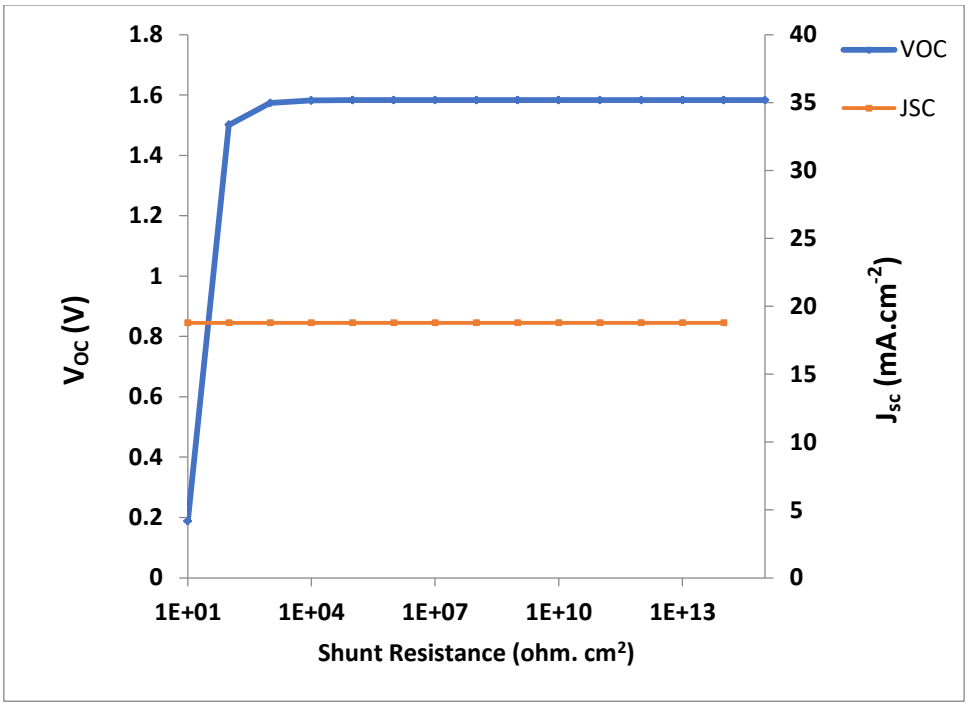

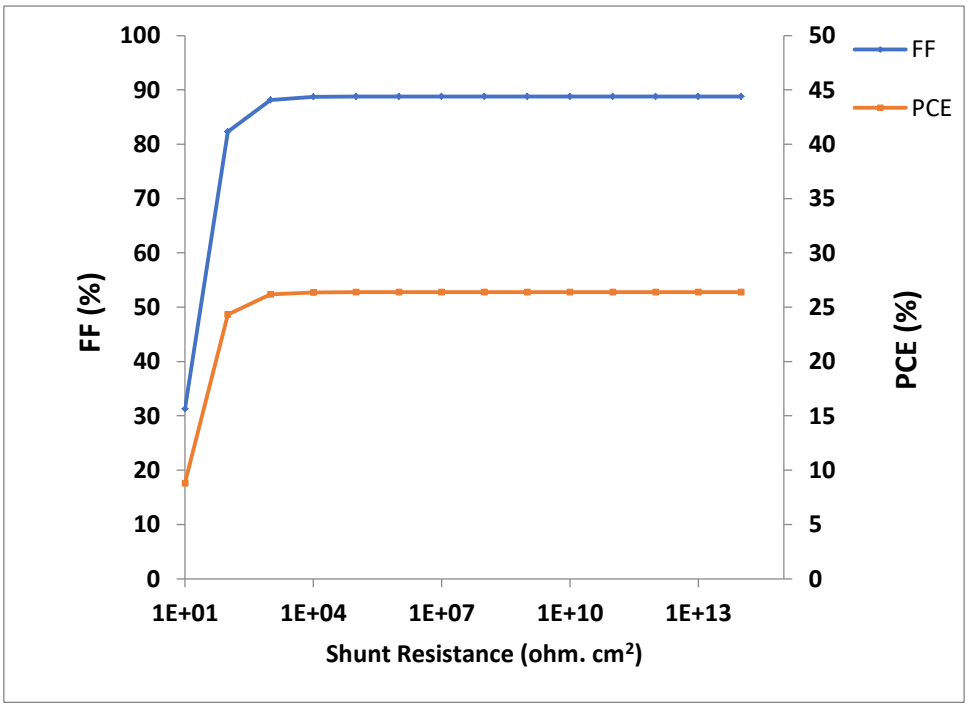

Fig. 12. Effect of the simulated parameters with the shunt resistance (colour online)

3.12. Effect of back contact

The back metal contact plays a crucial role in the performance of solar cell structures. Fig. 13 presents the effect of varying the electron work function of the back contact metal from 4.5 to 5.5 eV on the device's output characteristics. Initially, both the open-circuit voltage (V_{oc}) and power conversion efficiency (PCE) increase almost linearly as the work function rises from 4.5 to 5.3 eV. Beyond 5.3 eV, these parameters plateau and remain nearly constant up to 5.5 eV. Based on these simulation results, nikel, with an electron work function of 5.3 eV emerges as the most suitable replacement for gold as the back metal contact. This choice optimizes the solar cell's performance by maximizing voltage and efficiency, highlighting the importance of selecting appropriate electrode materials in device design.

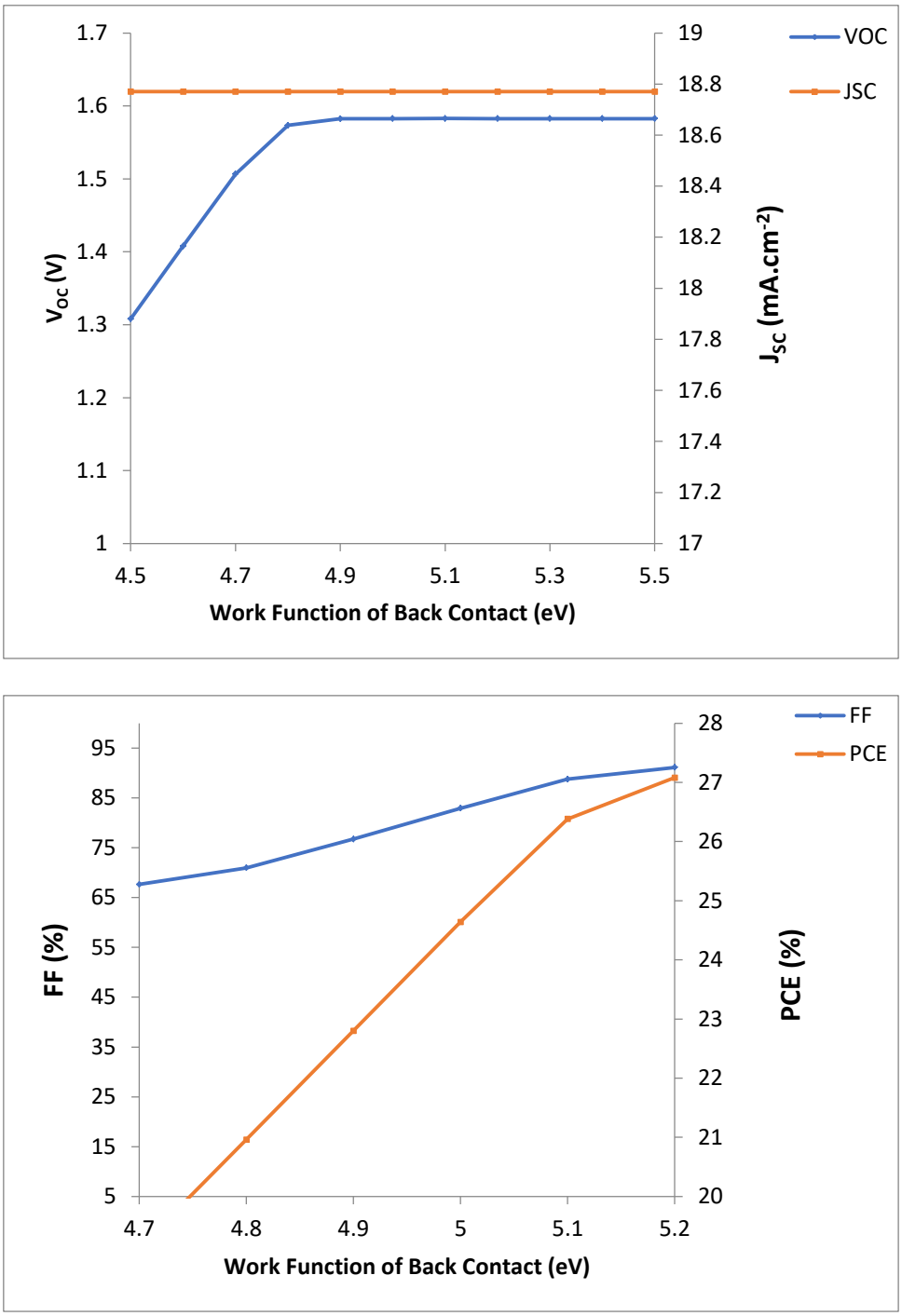

Fig. 13. Output parameters (V_{OC}, J_{SC}, FF, PCE) as a function of electron work function of back metal contact of the proposed solar cell structure (colour online)

3.13. Optimized device

The optimized parameters of the solar cell are summarized in Table 2. Fig. 14 presents the schematic of the optimized device alongside its current-voltage (J-V) characteristics curve, while Fig. 15 displays the quantum efficiency (QE) curve. The data indicate that the device efficiently absorbs a significant portion of visible light photons, making it suitable for solar energy applications. The optimized solar cell achieves a power conversion efficiency (PCE) of 26.38%, a fill factor (FF) of 88.78%, a short-circuit current density (J_{sc}) of 18.77 mA/cm², and an open-circuit voltage (V_{oc}) of 1.58 V. Table 3 compares these photovoltaic parameters with those of the initial device, demonstrating significant improvements through optimization.

Table 2. The optimized parameters of the device

Physical Parameters	**Symbol**	**Unit**	Spiro-OMeTAD **(HTL)**	**PEA_2PbI_4**	**ZnO:NR (ETL)**
Thickness	**Th**	nm	50	750	50
Uniform Shallow Donor Doping	**N_D**	cm^{-3}	0	1×10^{20}	1×10^{20}
Uniform Shallow Acceptor Doping	**N_A**	cm^{-3}	1×10^{20}	1×10^{18}	0
Defect Density	**N_t**	cm^{-3}	1×10^{15}	1×10^{15}	1×10^{15}

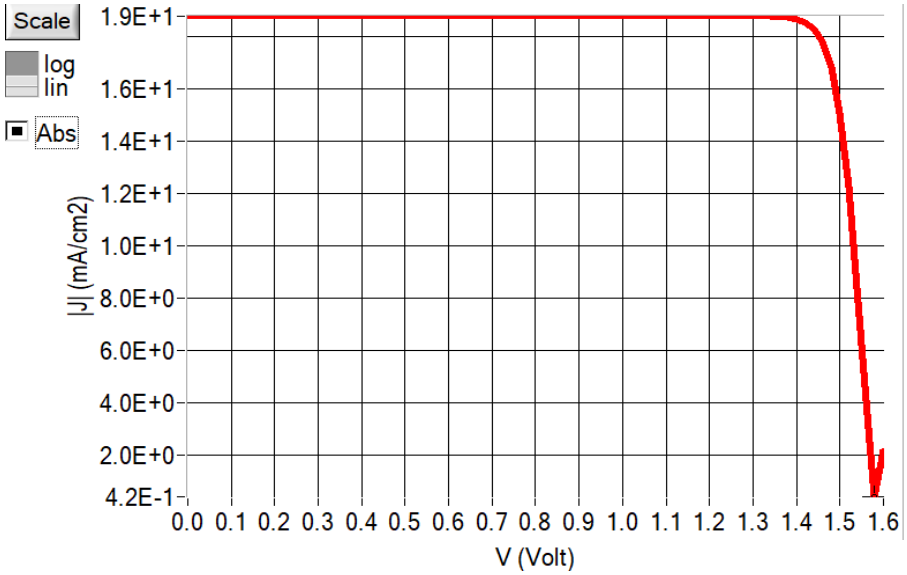

Fig. 14. Optimized device: J-V curve (colour online)

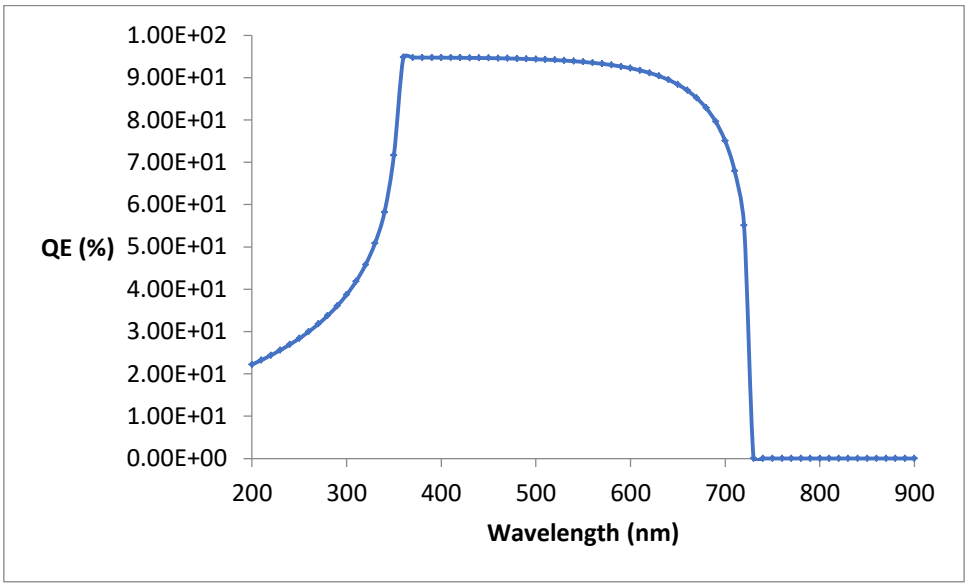

Fig. 15. QE of optimized device performance

Table 3. Output parameters of the optimized device and those of the initial one

Output parameters	PCE (%)	FF (%)	J_{SC} (mA/cm^2)	V_{OC} (V)
Initial device	20.06	80.94	17.54	1.41
Optimized device	26.38	88.78	18.77	1.58

4. Conclusion

This study presents a detailed numerical investigation into the performance enhancement of PEA_2PbI_4-based perovskite solar cells using SCAPS-1D simulation. By systematically varying the thicknesses, doping concentrations, and defect densities of the absorber (PEA_2PbI_4), ETL (ZnO:NR), and HTL (Spiro-OMeTAD), as well as environmental and electrical parameters such as temperature, series resistance, and shunt resistance, we identified an optimized configuration capable of delivering a maximum PCE of 26.38%. The optimal device also demonstrated excellent values for open-circuit voltage (1.58 V), short-circuit current density (18.77 mA/cm²), and fill factor (88.78%). These results underscore the critical role of interface engineering, material quality, and structural design in maximizing photovoltaic performance. Furthermore, the insights derived from this simulation study serve as a guiding framework for experimental realization and further development of efficient, stable, and scalable 2D perovskite solar cells suitable for real-world renewable energy applications.

Funding statement

This research did not obtain financial support from any specific grant provided by funding agencies in the public, commercial, or not-for-profit sectors.

Data availability statement

Data will be made available on request.

Declaration of interest's statement

The authors declare no conflict of interest.

Additional information

No additional information is available for this paper.

Acknowledgements

We would like to express our gratitude to Dr. Marc Burgelman and their team from Ghent University, Belgium, for providing access to the SCAPS simulator, which has been instrumental in conducting the simulations for this research.

Institutional Review Board Statement

Not applicable.

Informed Consent Statement

Not applicable.

References

[1] S. E. Smith, B. J. Stanislawski, B. K. Eng, N. Ali, T. J. Silverman, M. Calaf, R. B. Cal, Journal of Renewable and Sustainable Energy **14**(6), 063502 (2022).
[2] J. Clifton-Brown, K. U. Schwarz, D. Awty-Carroll, A. Iurato, H. Meyer, J. Greef, J. Gwyn, M. Mos, C. Ashman, C. Hayes, L. Huang, Agronomy **9**(11), 673 (2019).
[3] W. Zhang, H. He, H. Li, L. Duan, L. Zu, Y. Zhai, W. Li, L. Wang, H. Fu, D. Zhao, Advanced Energy Materials **11**(15), 2003303 (2021).
[4] C. Chen, X. Lu, B. Deng, X. Chen, Q. Guo, C. Li, C. Ma, S. Yuan, E. Sung, K. Watanabe, T. Taniguchi, Science Advances **6**(7), eaay6134 (2020).
[5] R. K. Shukla, A. Srivastava, S. Rani, N. Singh, V. K. Dwivedi, S. Pandey, N. Wadhwani, Nanosystems: Phys. Chem. Math. **15**(1), 135 (2024).
[6] Amrit Kumar Mishra, R. K. Shukla, Materials Today: Proceedings **46**, 2288 (2021).
[7] Amrit Kumar Mishra, R. K. Shukla, Materials Today: Proceedings **29**, 836 (2020).
[8] A. K. Mishra, R. K. Shukla, SN Applied Science **2**, 321 (2020).
[9] Q. Liu, Y. Sun, S. Wang, Q. An, L. Duan, G. Zhao, C. Wang, K. Doyle-Davis, H. Guo, X. Sun, Materials Today **64**, 21 (2023).
[10] Singh M. Gagandeep, R. Kumar, AIP Conf. Proc. **2115**, 030548 (2019).
[11] V. Nandal, P. R. Nair, ACS Nano **11**, 11505 (2017).
[12] Y. Du, H. Cai, H. Wen, Y. Wu, Z. Li, J. Xu, L. Huang, J. Ni, J. Li, J. Zhang, RSC Advances **6**, 83264 (2016).
[13] M. S. Shamna, K. S. Nithya, K. S. Sudheer, Materials Today: Proceedings **33**, 1246 (2020).
[14] Kunal Chakraborty, Sujubili Narzary, Priyanko Gohain, Samrat Paul, Sanat Das, Sreevardhan Cheerla, Prakash Kanakavalli, Journal of Nano- and Electronic Physics **16**, 1 (2024).
[15] Biplav Dahal, Melorina Dolafi Rezaee, Ram Chandra Gotame, Wenzhi Li, Materials Today Communications **36**, 106846 (2023).
[16] Qiong Zhang, Minglin Zhao, Yang Li, Ang Bian, Ramy El-Bashar, Hamdy Abdelhamid, Salah S. A. Obayya, Mohamed Farhat O. Hameed, Jun Dai, Opt. Express **32**, 25327 (2024).
[17] O. Daoudi, I. Jellal, A. Haddout, J. Zimou, O. El Khouja, K. Nouneh, M. Lharch, M. Fahoume, A.

Bendoumou, Journal of Materials Science: Materials in Electronics **34**(9), 819 (2023).
[18] C. Devi, R. Mehra, J. Mater. Sci. **54**, 5615 (2019).
[19] A. Bag, R. Radhakrishnan, R. Nekovei, R. Jeyakumar, Sol. Energy **196**, 177 (2020).
[20] G. Koishiyev, J. R. Sites, Sol. Energ. Mat. Sol. C **93**, 350 (2009).
[21] G. Xing, N. Mathews, S. Sun, S. Lim, Y. Lam, M. Grätzel, T. Sum, Science **342**, 344 (2013).
[22] L. Pazos-Outón, T. Xiao, E. Yablonovitch, J. Phys. Chem. Lett. **9**, 1703 (2018).

*Corresponding author: rajeshkumarshukla00@gmail.com